International Journal of New Technology and Research (IJNTR)
ISSN:2454-4116, Volume-3, Issue-12, December 2017 Pages 11-18

Computational Investigation of Cavitation on Horizontal Axis Tidal Turbines Blades

Douvi C. Eleni, Margaris P. Dionissios

Abstract— **This study will focus on the possibility of cavitation on various tidal turbine blades, constructed from four different airfoils, in particular a symmetrical airfoil, NACA 0024, and three cambered airfoils, Göttingen 770, NACA 4418 and NACA 4424. The optimum geometry of each rotor, in other words the chord length and the twist along the blade, is calculated by a user-friendly application based on the Blade Element Momentum method. This user-friendly application can also predict the power coefficient and the power output for tidal turbine rotors by examining different parameters, such as the hydrofoil profile for the blades, the number of blades, the tip speed ratio, the tidal current velocity and the rotor diameter. The flow over the optimum geometries was simulated by a commercial Computational Fluid Dynamics code for two different depths, three different blade lengths and at various tip speed ratios, in order to determine whether it is possible to occur cavitation under these operating conditions. The blade which experienced the less intense cavitation occurrence was the NACA 0024 blade.**

Index Terms— **Cavitation, optimum geometry, power output, tidal turbine.**

I. Introduction

The climate change has led to the development of renewable energy technologies, such as solar and wind, to generate electricity. Recently, researches have shown an increased interest in tidal turbine energy [1]–[6].

Although the design of the tidal turbines is like this of the wind turbines, they are more advantageous. The main advantage of tidal energy is that it is stable and predictable, in contrast to solar and wind energy. Furthermore, a tidal turbine can have the same nominal power with a wind turbine and at the same time the tidal turbine rotor is comparatively smaller and rotates at a lower speed, due to the greater density of seawater.

The performance of Horizontal Axis Tidal Turbines (HATT) can be predicted by the well-known Blade Element Momentum (BEM) method [7], [8], which was developed to predict the Horizontal Axis Wind Turbines (HAWT) performance.

A first systematic study of the HATT hydrodynamic performance prediction based on the BEM method was reported by Batten et al. in 2008 [9]. In 2011, Masters et al. [10] developed a BEM model, including corrections for losses at the tip and the hub of the blade. The results from this model were validated by comparison with a commercial code and a lifting line theory model. Chapman et al. [11] expanded the BEM model and included corrections for high induction conditions. More recently, Silva et al. [12] developed a BEM code with an innovative approach for the optimization of the blade geometry, considering the possibility of cavitation.

The main disadvantage of the BEM method is that it refers to two-dimensional flow, in other words it is not able to predict three-dimensional phenomena that occur in real flow. Several studies investigating the hydrodynamic performance of HATTs based on the BEM method and computational fluid dynamics have been carried out [13]-[17].

The most significant problem during the operation of a tidal turbine is the occurrence of cavitation, which is caused by the interaction of the rotating blades with seawater. Cavitation should be avoided because it could even lead to failure of the blades.

In 2015, Zhang et al. [18] conducted numerical simulations and showed that the location and extend of cavitation on the blade are affected by tip speed ratio. They also showed that the hydrodynamic performance of the HATT degrades when cavitation area extends in the middle of blade. At the same time, Wang et al. [19] designed and simulated a 50 kW HATT blade and found that cavitation started from the tip and expanded to the middle of the blade. Jung and Kim [20] designed and investigated computationally a two bladed HATT rotor with S814 airfoil profile and observed cavitation on both suction and pressure sides of the blade. In 2016, Gharraee et al. [21] carried out numerical simulations with the ReFRESCO viscous flow solver and demonstrated that the possibility of cavitation occurrence on the blades is higher for tidal turbines mounted on floating structures than for seabed mounted tidal turbines.

The performance of a HATT is affected mainly by the geometry of the blades, i.e. the selected hydrofoil profiles and the chord and twist distribution along the blade. The aim of this study is to examine the occurrence of cavitation under different blade lengths and different conditions.

Firstly, the optimum geometries of the blades are calculated by a user-friendly application [22]. Then, the blades with these geometrical characteristics are designed in QBlade software [23] and finally they are simulated numerically by a commercial Computational Fluid Dynamics (CFD) code. The occurrence of cavitation, which can cause even failure of the blade, is examined.

Eleni C. Douvi, Department of Mechanical Engineering and Aeronautics, University of Patras, Patras, Greece
Dionissios P. Margaris, Department of Mechanical Engineering and Aeronautics, University of Patras, Patras, Greece
This work was supported by the Greek State Scholarships Foundation (IKY), Fellowships of Excellence for Postdoctoral Studies (Siemens Program).

II. NUMERICAL ANALYSIS

A. *Design of Optimum Geometry*

The first step in the simulation procedure is the design of the tidal turbine blade. The optimum geometry, the power output and the power coefficient of the HATT rotors were calculated by a user-friendly application developed by Douvi and Margaris [22], based on the BEM theory. This application is novel and has the advantage that it can give reliable results in low computational time and memory. Moreover, it can be used for Horizontal Axis Wind Turbines as well, just by changing the seawater density with the air density. The form of the application is presented in Fig. 1.

Fig. 1. The form of the user-friendly application based on BEM method.

Values regarding the rotor diameter and the number of blades, hydrofoil sections and elements along the blade, the tip speed ratio, the tidal current velocity, the hydrodynamic characteristics and the corresponding angle of attack of the selected hydrofoils can be entered by the user.

The lift and drag coefficients of the hydrofoils, that should be entered by the user, correspond to the values at the optimum angle of attack in which the lift to drag ratio reaches the highest value. The prediction of the hydrodynamic coefficients of the selected hydrofoils at various angles of attack is accomplished by the QBlade software [23], which is integrated with the XFOIL for airfoil design and analysis. Once the hydrofoil characteristics are predicted, the lift to drag ratio can be calculated.

Four airfoils were selected as candidate solutions, specifically Göttingen 770, NACA 0024, NACA 4418 and NACA 4424. NACA 0024 airfoil is symmetrical and its maximum thickness is 24% of chord length. The remaining three airfoils have 4% camber, Göttingen 770 at 30% and NACA 4418 and NACA 4424 at 40% of the chord length. The maximum thickness for the Göttingen 770, NACA 4418 and NACA 4424 is 21% 18% and 24% of chord length respectively. The optimum angle of attack and the corresponding aerodynamic coefficients for these airfoils are illustrated in Table I.

Since there was no significant difference between three-bladed and four-bladed rotors, due to lower cost of construction a three-bladed rotor is preferable, so only three-bladed rotors were examined [22]. The rotor diameter for the calculations of the optimum geometry was 10m, a typical value suggested for some of the devices for the

Table I. Aerodynamic coefficients at the optimum angle of attack for the airfoils.

Airfoil type	**Optimum Characteristics**		
	Angle of attack	***Lift coefficient, C_l***	***Drag coefficient, C_d***
GOE 770	8.5	1.2509	0.01255
NACA 0024	11.0	1.1543	0.01056
NACA 4418	7.0	1.2378	0.00885
NACA 4424	7.0	1.1763	0.00922

Alderney Race [24,25]. The performance of the HATT rotors was firstly calculated at tip speed ratios ranging from 4 to 14 and then the tip speed ratio corresponding to the higher power coefficient was entered for the calculation of the optimum geometry.

The optimum blade geometries were designed in the QBlade software [23], which was developed for the design and simulation of horizontal and vertical wind turbines. The design of the rotor blades and the corresponding airfoil sections are presented in Fig. 2 and Fig. 3.

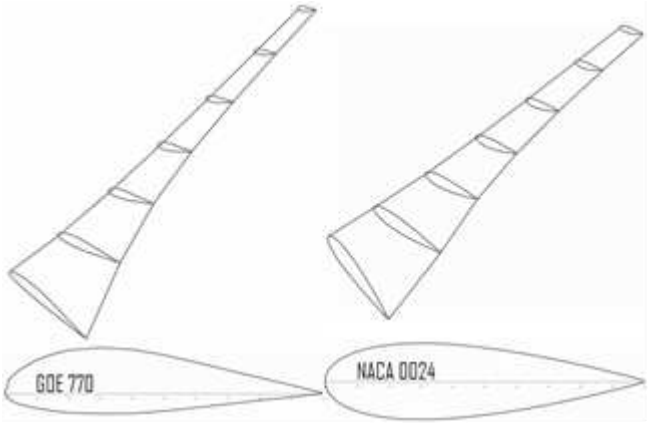

Fig. 2. HATT blade optimum design with Göttingen 770 (GOE 770) airfoil and GOE 770 airfoil (left) and HATT blade optimum design with NACA 0024 airfoil and NACA 0024 airfoil (right).

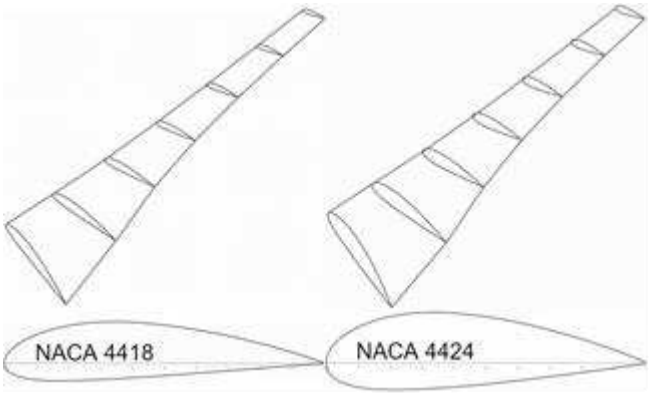

Fig. 3. HATT blade optimum design with NACA 4418 airfoil and NACA 4418 airfoil (left) and HATT blade optimum design with NACA 4424 airfoil and NACA 4424 airfoil (right).

B. *Computational Method*

The commercial CFD code ANSYS Fluent [26] was used to predict the hydrodynamic behavior of the HATT rotors and

the cavitation occurrence. The HATT rotors that were simulated are three-bladed rotors with a diameter of 5m, 10m and 15m and different hydrofoil profiles were used for the blades. It should be noted that the optimum geometry that was calculated, as described in the previous section, was used for all the simulations, since it is not feasible to construct different blades for all tip speed ratios. Simulations were conducted for various tip speed ratios and two different water depths. The hub is located 20m and 60m below the surface, in a sufficient depth that commercial navigation will not be affected.

To gain computational time, only the volume mesh around a single blade of the three-bladed rotor was generated, with a periodicity of 120 degrees. The remaining two blades of the HATT rotor were included to the computations by applying periodic boundary conditions. The tower and the hub of the HATT were completely removed from the simulations, since their effect on the rotor dynamics is negligible [27].

One third of a horizontally placed truncated cone was selected to be the computational domain over the blade. The front and the lateral side of the truncated cone are defined as velocity inlet, the rear side as pressure outlet and the blade as wall. The velocity inlet was located upstream the rotor in a distance that is twice the blade length. Similarly, the radius of the cone at the velocity inlet was also set equal to twice the blade length. The pressure outlet was four times the blade length downstream the rotor and the cone radius at the pressure outlet was three times the blade length. Fig. 4 presents the computational domain and the boundary conditions.

The blade was structurally meshed, an inflation was added over the blade and the mesh over the single blade was unstructured. Close to the blade, where greater computational accuracy is needed due to the changes in the flow, the mesh was denser.

The most appropriate turbulence model for current simulations, where Reynolds numbers are high, is the standard k-ε model [28]. The Moving Reference Frame Model (MRF) [29] was used to simulate the rotation of the blades.

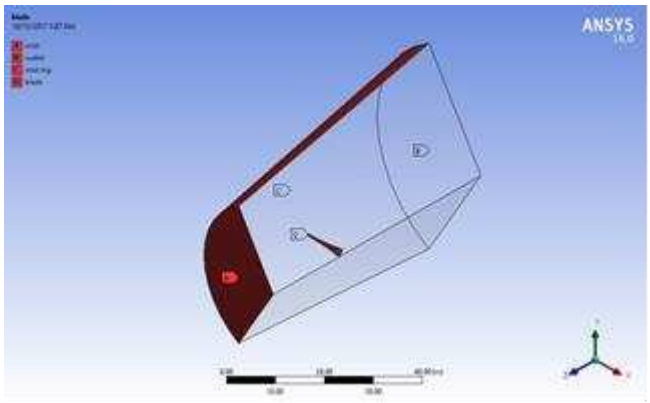

Fig. 4. Computational domain and boundary conditions around the HATT blade.

A two-phase continuous mixture of seawater and vapor was considered for the simulation of the cavitation flows. The Zwart-Gerber-Belamri cavitation model [30], which is based on the simplified Rayleigh-Plesset equation [31], was included in the simulations. A typical value of seawater density is about 1025 kg/m^3 and the vaporization pressure of seawater is 2291 Pa.

III. RESULTS AND DISCUSSION

The power output results obtained from the user-friendly, based on the BEM method, application and the commercial CFD code for the tip speed ratio number with the higher performance are presented in Table II. It can be seen from these data that there is a good agreement between the values of the power output obtained by the application and the CFD code, since the mean error was found to be about 4.5%. From these data it is apparent that the optimum tip speed ratio is low and has almost the same value for all the examined blades.

Table II. Power output at optimum tip speed ratio.

Airfoil type	***Tip Speed Ratio***	**Power Output (MW)**		***Error (%)***
		BEM application	***CFD code***	
GOE 770	4.5	2.352	2.246	4.5
NACA 0024	4.5	2.362	2.232	5.5
NACA 4418	4.5	2.385	2.309	3.2
NACA 4424	4.0	2.373	2.495	5.1

Cavitation occurrence was examined for blades of 5m, 10m and 15m length. The cavitation was quantified by the total volume of the vapor. The shorter blades, these of 5m, did not experience cavitation.

The Göttingen 770 blade was the only blade that experienced cavitation in the depth of 60m, as it can be seen from Fig. 5. For this case, cavitation occurred only at the pressure side of the blade, close to the tip and the leading edge.

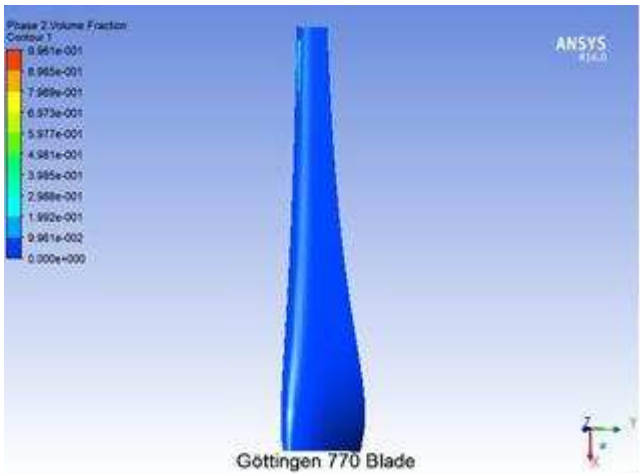

Fig. 5. Cavitation on the pressure side of Göttingen 770 blade of 15m length, at tip speed ratio equal to 8 and location of the hub 60m below the sea surface.

Fig. 6 to Fig. 12 show the cavitation on both pressure and suction sides of the Göttingen 770 blade for hub submersion depth of 20m and various tip speed ratios.

In general, from these results it is obvious that at the pressure side of the blade cavitation occurs near the tip of the blade at the leading edge, and as the tip speed ratio increases

cavitation area extents to the middle of the blade. On the other hand, at the suction side of the blade, cavitation occurs close to the tip and the trailing edge.

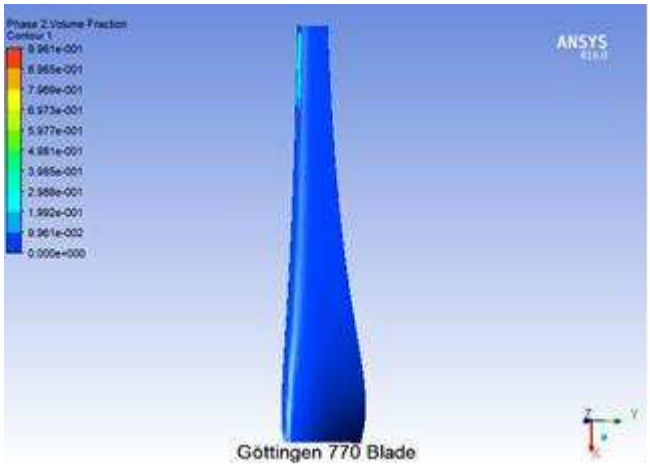

Fig. 6. Cavitation on the pressure side of Göttingen 770 blade of 10m length, at tip speed ratio equal to 8 and location of the hub 20m below the sea surface.

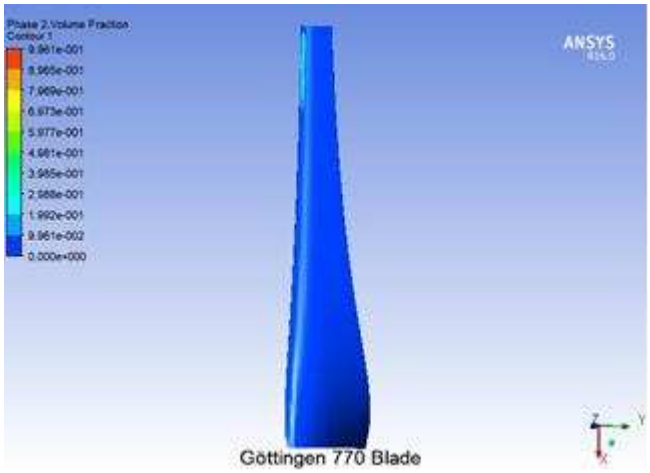

Fig.7. Cavitation on the pressure side of Göttingen 770 blade of 15m length, at tip speed ratio equal to 6 and location of the hub 20m below the sea surface.

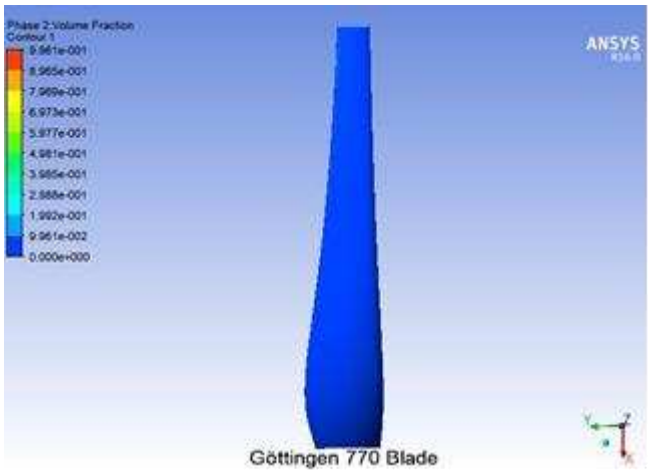

Fig. 8. Cavitation on the suction side of Göttingen 770 blade of 15m length, at tip speed ratio equal to 6 and location of the hub 20m below the sea surface.

More specifically, for a tip speed ratio equal to 8 and blade length of 10m cavitation hardly occurs only at the pressure side of the blade. Regarding the longer blade of 15m, cavitation on the pressure side of the blade appears at a lower tip speed ratio equal to 6, while at the suction side of the blade cavitation hardly occurs. As the tip speed ratio increases cavitation is more intense. In particular, the cavitation area extents towards the hub of the blade and covers larger area from the trailing edge to the middle of the hydrofoil.

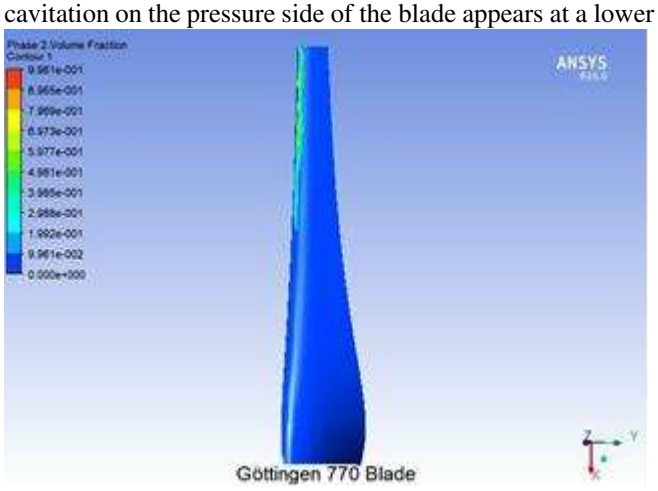

Fig. 9. Cavitation on the pressure side of Göttingen 770 blade of 15m length, at tip speed ratio equal to 7 and location of the hub 20m below the sea surface.

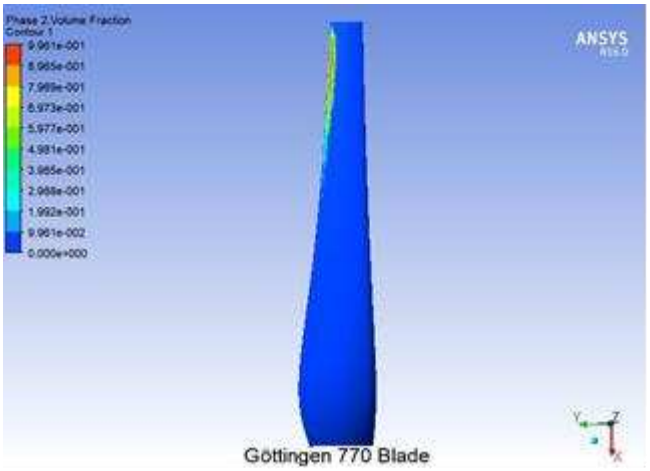

Fig. 10. Cavitation on the suction side of Göttingen 770 blade of 15m length, at tip speed ratio equal to 7 and location of the hub 20m below the sea surface.

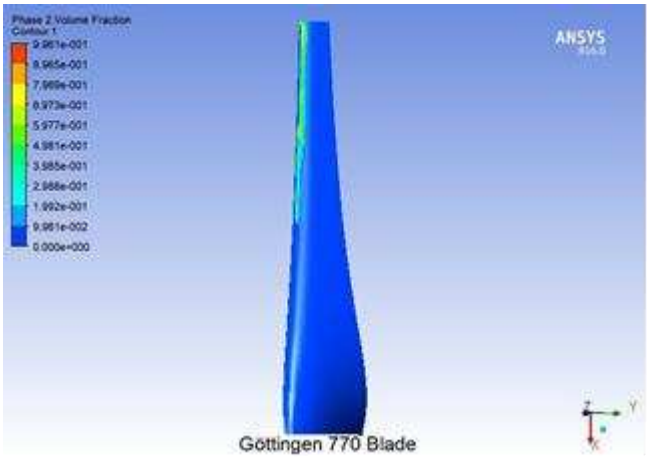

Fig. 11. Cavitation on the pressure side of Göttingen 770 blade of 15m length, at tip speed ratio equal to 8 and location of the hub 20m below the sea surface.

Fig. 13 and Fig. 14 show the cavitation on the pressure and the suction area of the 15m long NACA 0024 blade respectively, at TSR=8. At this tip speed ratio, the 10m long NACA 0024 blade did not experience cavitation. Compared with the corresponding results of Göttingen 770 blade (Fig. 11 and Fig. 12), it is apparent that on the NACA 0024 blade pressure side cavitation occurs at the same location, but covers smaller area. At the suction side of the same blade (Fig. 14), cavitation is less intense and occurs close to the tip and the leading edge.

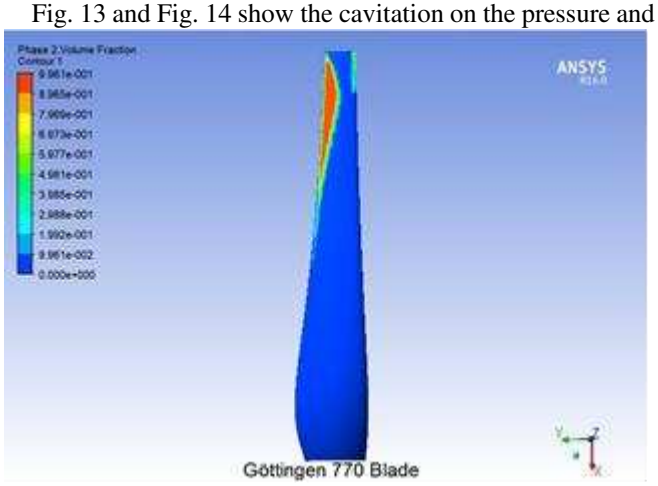

Fig. 12. Cavitation on the suction side of Göttingen 770 blade of 15m length, at tip speed ratio equal to 8 and location of the hub 20m below the sea surface.

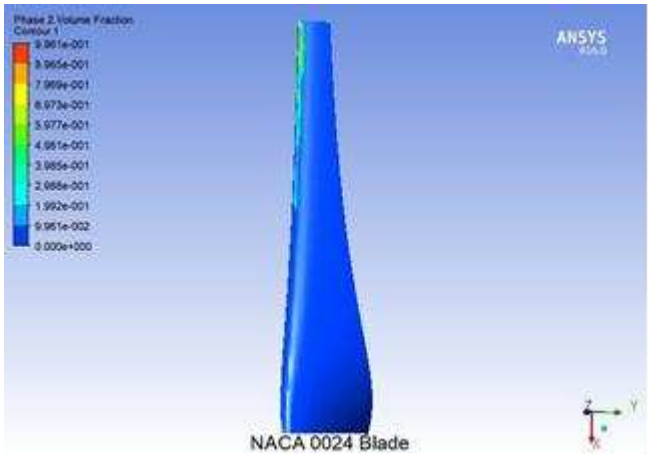

Fig. 13. Cavitation on the pressure side of NACA 0024 blade of 15m length, at tip speed ratio equal to 8 and location of the hub 20m below the sea surface.

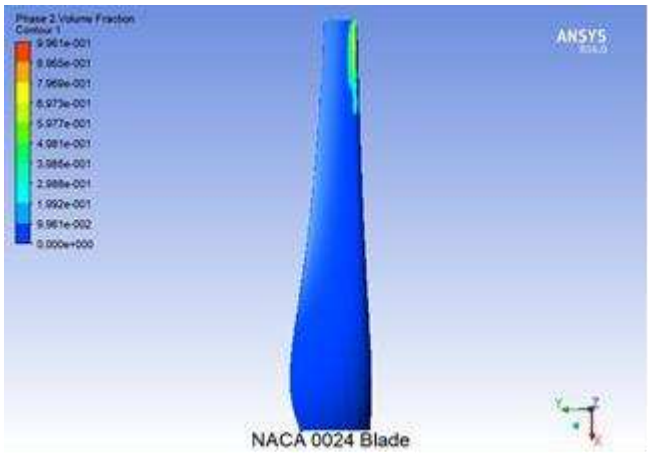

Fig. 14. Cavitation on the suction side of NACA 0024 blade of 15m length, at tip speed ratio equal to 8 and location of the hub 20m below the sea surface.

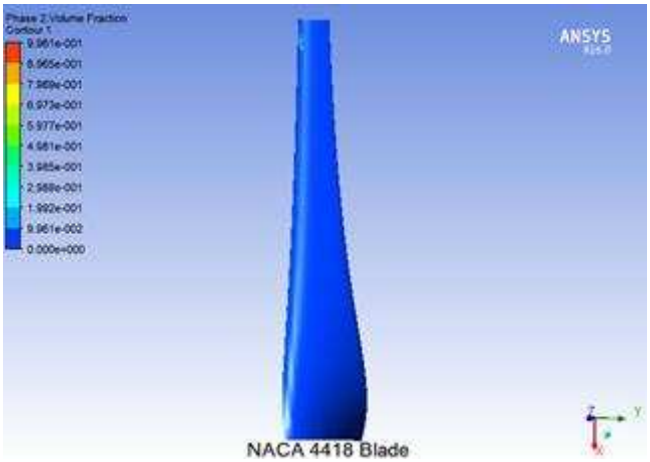

Fig. 15. Cavitation on the pressure side of NACA 4418 blade of 10m length, at tip speed ratio equal to 8 and location of the hub 20m below the sea surface.

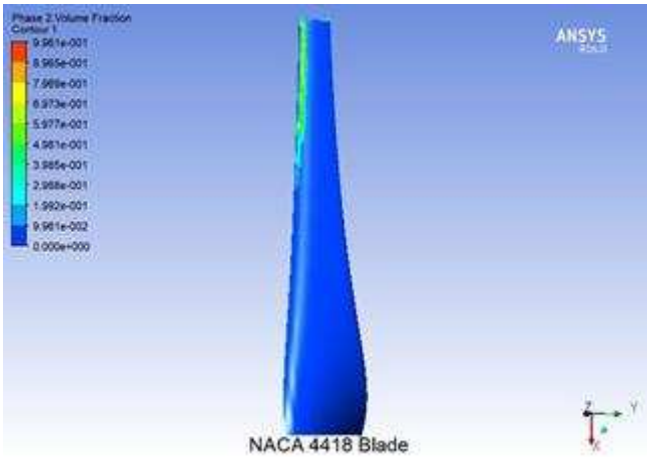

Fig. 16. Cavitation on the pressure side of NACA 4418 blade of 15m length, at tip speed ratio equal to 8 and location of the hub 20m below the sea surface.

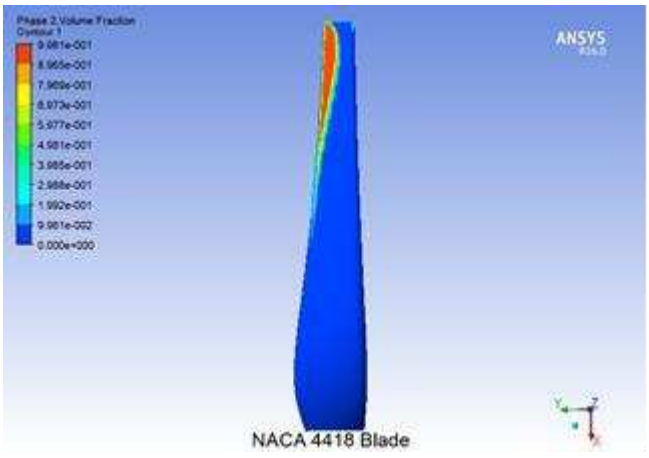

Fig. 17. Cavitation on the suction side of NACA 4418 blade of 15m length, at tip speed ratio equal to 8 and location of the hub 20m below the sea surface.

Fig. 15 to Fig. 20 present the cavitation occurrence on the pressure and suction sides of NACA 4418 and NACA 4424 blades. As the thickness of the blade with the NACA 44-series airfoil profile increases, the cavitation area

increases on both sides of the blade. Moreover, for blades of 10m cavitation starts to occur close to the blade tip at a tip speed ratio of 8, although for longer blades cavitation starts at lower tip speed ratios.

The NACA 4424 blade experience the most intense cavitation among the examined blades. The cavitation patterns of NACA 4418 blade and Göttingen 770 blade are

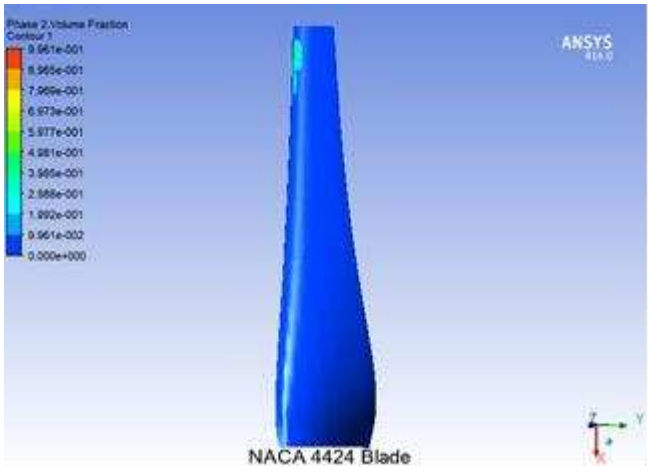

Fig. 18. Cavitation on the pressure side of NACA 4424 blade of 10m length, at tip speed ratio equal to 8 and location of the hub 20m below the sea surface.

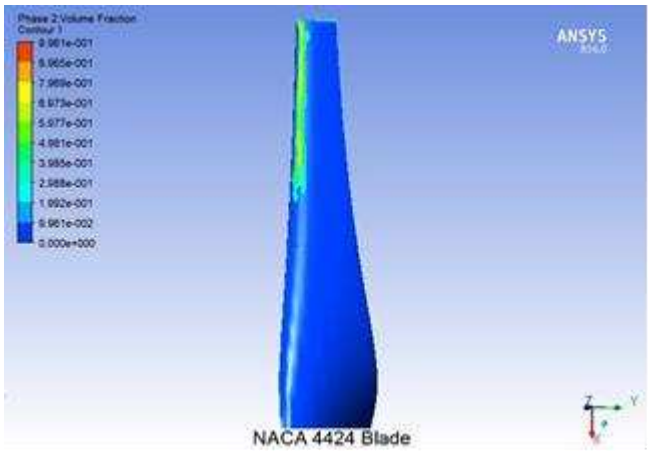

Fig. 19. Cavitation on the pressure side of NACA 4424 blade of 15m length, at tip speed ratio equal to 8 and location of the hub 20m below the sea surface.

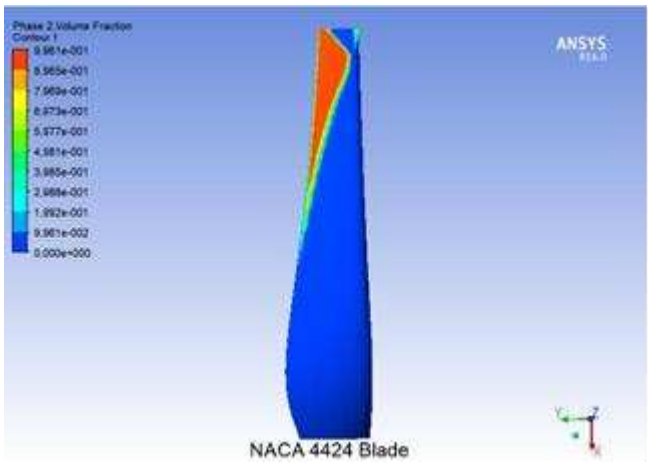

Fig. 20. Cavitation on the suction side of NACA 4424 blade of 15m length, at tip speed ratio equal to 8 and location of the hub 20m below the sea surface.

similar, but further statistical analysis revealed that on the NACA 4418 blade exists larger volume of vapor than on the Göttingen 770 blade.

Fig. 21 presents the volume fraction of the vapor on the blade for 15m long blades and at a tip speed ratio of 8. It should be noted that the blades have also the same behavior for lower values of tip speed ratio when cavitation occurs. For instance, the 4424 blade experiences the most intense cavitation and the NACA 0024 blade experience the least intense cavitation.

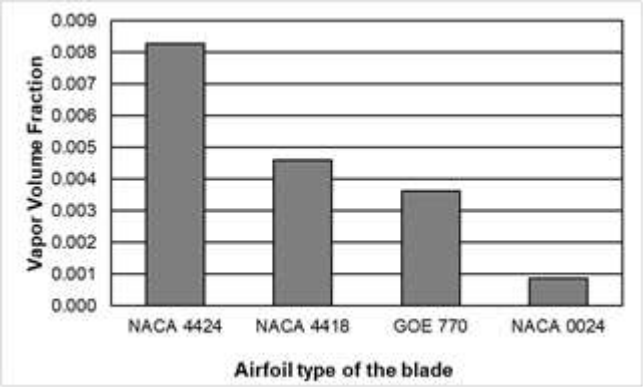

Fig. 21. Vapor volume fraction on the examined blades of 15m length, at tip speed ratio equal to 8 and location of the hub 20m below the sea surface.

Summarizing, the occurrence of cavitation is related to the depth of tidal turbine submersion, the length of the blade, the tip speed ratio number as well as the hydrofoil profile of the blade. In general, cavitation occurs at smaller depths, longer blades and higher tip speed ratios. Furthermore, since the NACA 0024 blade has the best behavior under cavitation, it can be concluded that the camber of the hydrofoil profile has a negative effect in cavitation occurrence.

IV. Conclusion

The present study was designed to examine the cavitation occurrence on different horizontal axis tidal turbine blades, which operate under different conditions. The optimum geometries of the blades were calculated, designed and simulated numerically by a commercial Computational Fluid Dynamics code. The computational results for the power output agreed with the numerical results obtained from the user-friendly application based on the BEM method.

From the volume fraction of the vapor on the blade, conclusions about the cavitation occurrence derived and it was concluded that the depth of tidal turbine submersion is a significant factor that affects this phenomenon. Cavitation was found to occur at smaller depths and at the depth of 60m only the Göttingen 770 blade experienced cavitation.

Other factors that affect cavitation are the blade length and the tip speed ratio. Cavitation tends to occur at longer blades and at higher values of tip speed ratio. In general, cavitation occurred close to the tip of the blade and as the tip speed ratio increased the cavitation area was growing on both sides of the blades.

The examined blades can be classified from this that experienced the least to this that experienced the most intense

cavitation as: NACA 0024, Göttingen 770, NACA 4418 and NACA 4424 blade. The most significant finding to emerge from this study is that the camber of the hydrofoil profile has a negative effect in cavitation occurrence, therefore symmetrical airfoils seem to be more appropriate for HATT rotors.

It is recommended that further research be undertaken to improve the blade geometry close to the tip, in order to reduce the possibility of cavitation occurrence. The investigation of various types of hydrofoils as candidate sections along the blade would be very interesting.

ACKNOWLEDGMENT

This work was supported by the Greek State Scholarships Foundation (IKY), Fellowships of Excellence for Postdoctoral Studies (Siemens Program).

REFERENCES

[1] F.O. Rourke, F. Boyle, and A. Reynolds, "Marine current energy devices: Current status and possible future applications in Ireland," Renewable and Sustainable Energy Reviews, Vol. 14(3), pp. 1026-1036, 2010.
[2] A.S. Bahaj, "Generating electricity from the oceans," Renewable and Sustainable Energy Reviews, Vol. 15(7), pp. 3399-3416, 2011.
[3] K.W. Ng, W.H. Lam, and K.C. Ng, "2002-2012: 10 years of research progress in horizontal-axis marine current turbines," Energies, Vol. 6(3), pp. 1497-1526, 2013.
[4] T.A.A. Adcock, S. Draper, and T. Nishino, "Tidal power generation - A review of hydrodynamic modelling," Proceedings of the Institution of Mechanical Engineers, Part A: Journal of Power and Energy, Vol. 229(7), pp. 755-771, 2015.
[5] L. Zhang, J. Shang, Z. Zhang, J. Jiang, and X. Wang, "Tidal current energy update 2015 -Hydrodynamics," Shuili Fadian Xuebao/Journal of Hydroelectric Engineering, Vol. 35(2), pp. 1-15, 2016.
[6] N.D. Laws, and B.P. Epps, "Hydrokinetic energy conversion: Technology, research, and outlook," Renewable and Sustainable Energy Reviews, Vol. 57, pp. 1245-1259, 2016.
[7] H. Glauert, "A General Theory of the Autogyro," ARCR R&M, Vol. 1111, pp. 558 –593, 1926.
[8] S. Wang, C. Chen, J. Tan, P. Yuan, and X. Zhou, "Hydrodynamic performance of horizontal axis tidal current turbine based on blade element momentum theory," Taiyangneng Xuebao/Acta Energiae Solaris Sinica, Vol. 35, pp. 599–604, 2014.
[9] W.J. Batten, A. Bahaj, A. Molland, and J. Chaplin, "The prediction of the hydrodynamic performance of marine current turbines," Renewable Energy, Vol. 33, pp. 1085–1096, 2008.
[10] I. Masters, J. Chapman, M. Willis, and J. Orme, "A robust Blade Element Momentum Theory model for tidal stream turbines including tip and hub loss corrections," Journal of Marine Engineering and Technology, Vol. 10, pp. 25–35, 2011.
[11] J. Chapman, I. Masters, M. Togneri, and J.A. Orme, "The Buhl correction factor applied to high induction conditions for tidal stream turbines," Renewable Energy, Vol. 60, pp. 472–480, 2013.
[12] P.A.S.F. Silva, L.D. Shinomiya, T.F. de Oliveira, J.R.P. Vaz, A.L. Amarante Mesquita, and A.C.P. Brasil Junior, "Analysis of cavitation for the optimized design of hydrokinetic turbines using BEM," Applied Energy, Vol. 185, p. 1281-1291, 2017.
[13] J.H. Lee, S. Park, D.H. Kim, S.H. Rhee, and M.C. Kim, "Computational methods for performance analysis of horizontal axis tidal stream turbines," Applied Energy, Vol. 98, pp. 512-523, 2012.
[14] M.C. Kim, I.R. Do, S.H. Rhee, B.S. Hyun, and M.S. Song, "Numerical investigation on the performance of 1-MW class tidal current horizontal axis turbines," Proceedings of the International Offshore and Polar Engineering Conference, pp. 757-762, 2012.
[15] R. Malki, A.J. Williams, T.N. Croft, M. Togneri, and I. Masters, "A coupled blade element momentum - Computational fluid dynamics model for evaluating tidal stream turbine performance", Applied Mathematical Modelling, Vol. 37(5), pp. 3006-3020, 2013.
[16] Q. Sheng, D. Zhao, and L. Zhang, "A design and numerical simulation of horizontal tidal turbine," Harbin Gongcheng Daxue Xuebao/Journal of Harbin Engineering University, Vol. 35(4), pp. 389-394, 2014.
[17] P.M. Singh, and Y.D. Choi, "Shape design and numerical analysis on a 1MW tidal current turbine for the south-western coast of Korea," Renewable Energy, Vol. 68, pp. 485-493, 2014.
[18] L. Zhang, L. Fang, and X. Zhang, "Study on cavitation characteristics of horizontal axis tidal turbine," Huazhong Keji Daxue Xuebao (Ziran Kexue Ban)/Journal of Huazhong University of Science and Technology (Natural Science Edition), Vol. 43(2), pp. 50-54, 2015.
[19] S. Wang, C. Sheng, P. Yuan, J. Tan, and K. Zhang, "Numerical simulation of cavitation on horizontal axis tidal current turbine," Taiyangneng Xuebao/Acta Energiae Solaris Sinica, Vol. 36(2), pp. 522-528, 2015.
[20] J.H. Jung, and B.S. Kim, "Rotor-blade shape design and power-performance analysis for horizontal-axis tidal turbine using CFD," Transactions of the Korean Society of Mechanical Engineers, Vol. 39(8), pp. 661-668, 2015.
[21] B. Gharraee, C. Eskilsson, R. Bensow, and G. Vaz, "Numerical simulation of cavitation on a horizontal axis tidal turbine," Proceedings of the International Offshore and Polar Engineering Conference, pp. 709-716, 2016.
[22] E. Douvi, and D. Margaris, "Hydrodynamic Analysis of a Horizontal Axis Tidal Turbine, Based on the Blade Element Momentum Theory," Proceedings of the 7th International Conference on "Experiments/ Process/ System Modeling/ Simulation/ Optimization, 2017.
[23] D. Marten, J. Wendler, G. Pechlivanoglou, C.N. Nayeri, and C.O. Paschereit, "QBlade: An Open Source Tool for Design and Simulation of Horizontal and Vertical Axis Wind Turbines," International Journal of Emerging Technology and Advanced Engineering, Vol. 3, pp. 264–269, 2013.
[24] L.S. Blunden, and A.S. Bahaj, "Tidal energy resource assessment for tidal stream generators," Proceedings of the Institution of Mechanical Engineers, Part A: Journal of Power and Energy, Vol. 221, pp. 137–146, 2007.
[25] L.E. Myers, and A.S. Bahaj, "Simulated electrical power potential harnessed by marine current turbine arrays in the Alderney Race," Renewable Energy, Vol. 30, pp. 1713–1731, 2005.
[26] ANSYS® Academic Research, Release 16.0
[27] M. Edmunds, R. Malki, A.J. Williams, I. Masters, and T.N. Croft, "Aspects of tidal stream turbine modelling in the natural environment using a coupled BEM-CFD model," International Journal of Marine Energy, Vol. 7, pp. 20-42, 2014.
[28] B.E. Launder, and D.B. Spalding, Lectures in Mathematical Models of Turbulence, Academic Press, London, England, 1972.
[29] J.Y. Luo, R.I. Issa, A.D. Gosman, "Prediction of Impeller–Induced Flows in Mixing Vessels Using Multiple Frames of Reference," In IChemE Symposium Series 1994, pp. 549–556, 1994.
[30] P.J. Zwart, A.G. Gerber, and T.Belamri, "A Two-Phase Flow Model for Predicting Cavitation Dynamics," In Fifth International Conference on Multiphase Flow, Yokohama, Japan, 2004.
[31] C.E. Brennen, Cavitation and Bubble Dynamics, Oxford University Press, 1995.

Eleni C. Douvi, born in Korinthos, Greece on March 15th, 1984. She is a post-doctoral researcher of the Mechanical Engineering and Aeronautics Department at University of Patras. Her research activity is the proposal of the optimum geometry of a horizontal axis tidal turbine rotor. Her doctoral thesis was experimental and computational investigation of aerodynamic behavior of wings in heavy rain, applied to horizontal axis wind turbine blades. In her diploma thesis was dealing with the experimental study of fluid mechanics applying LDA and PDA measurements. She is participating in 13 international conferences on the above scientific areas and has 6 publications on high-interested impact factor Journals.

Dionissios P. Margaris, born in Zakynthos island, Greece on September 28th, 1953. He is Professor in Mechanical Engineering and Aeronautics Department at the University of Patras, Patras, Greece. His research activities/fields are multiphase flows of gas-liquid-solid particles, gas-liquid two-phase flow air-lift pump performance, centrifugal and T-junction separation modeling in gas-liquid two-phase flow, experimental and theoretical investigation of hot air dehydration of agricultural products, experimental and theoretical investigation of capillary pumped loops, steady and transient flows in pipes and network and numerical simulation of centrifugal pump performance.

Also he is dealing with fluid dynamics analysis of wind turbines and aerodynamic installations, aero-acoustic analysis and environmental impacts of wind turbines. He is participating in over 130 international conferences on the above scientific areas and has over 80 publications on high-interested impact factor Journals. Prof. Dionissios P. Margaris is participating in several research projects supported by HAI, GSRT, CEC-THERMIE. Also he is member of AIAA, AHS, ASME and EUROMECH unions as well as of TCG (Technical Chamber of Greece).